# CHARACTERISTICS OF THE STRONG GROUND MOTIONS FROM THE 2018 HOKKAIDO EASTERN IBURI EARTHQUAKE FROM THE ANALYSIS OF HIGH-DENSITY STRONG GROUND MOTION DATA

Y. Kakehi[1]

[1] *Research Associate, Graduate School of Science, Kobe University, kakehi@kobe-u.ac.jp*

## Abstract

Characteristics of the strong ground motions from the 2018 Hokkaido Eastern Iburi earthquake ($M_W$ 6.6, 37.0 km depth, called "event 1" hereafter) are studied using the records of high-density strong ground motion observation network (NIED K-NET and KiK-net). In this study, spatial contrast of high-frequency seismic wave amplitude between the forearc and backarc sides of the island arc, caused by the decay of high-frequency waves in the backarc side due to propagating low-Q medium is focused on. For comparison, strong ground motions from two other deeper earthquakes, the 2015 interplate earthquake ($M_W$ 6.1, 66.07 km, event 2) and the 2007 intraslab earthquake ($M_W$ 5.5, 126.18 km, event 3), are also analyzed. From the analysis of the spatial distribution of peak ground acceleration, trace of wave propagation along linear arrays, and attenuation relation of peak ground acceleration, the spatial contrast of high-frequency wave amplitude between the forearc and backarc sides is found to be clear for the two deeper events (event 2 and 3), but is not clear for the shallowest event 1. This result is interpreted by referring to the following two factors. The first factor is the path length of seismic waves propagating in low-Q medium in the backarc side. The path length of the shallowest event 1 is shorter than those of the two deeper events, and this makes the decay of high-frequency wave amplitude in the backarc side unclear for event 1. The second factor is the spatial variation of geometrical spreading factor. The spatial variation of geometrical spreading factor of the shallowest event 1 is stronger than those of the two deeper events. This works as a mask effect to the spatial contrast between the forearc and backarc sides originated from the heterogeneous attenuation structure in case of event 1. In Hokkaido, since the attenuation structure is relatively complex due to the existence of the low-Q zone in the western side of Hidaka collision zone in the forearc side, the spatial distribution of high-frequency wave amplitudes also becomes relatively complex for all of the three events.

*Keywords: 2018 Hokkaido Eastern Iburi earthquake, strong ground motion, attenuation, island arc*

## 1. Introduction

An $M_W$ 6.6 earthquake occurred on 6 September 2018 in Hokkaido, Japan. This earthquake was named "2018 Hokkaido Eastern Iburi earthquake" by the Japan Meteorological Agency. It occurred in the region called "Hidaka collision zone", where the Kuril arc collides with the northeastern Japan arc (Fig. 1). The underground structure beneath Hidaka collision zone is complex due to the arc-arc collision, and inland earthquakes occur with much deeper focal depths than those of normal inland earthquakes (Kita et al., 2014 [1]).

In this study, characteristics of the strong ground motions by the 2018 Hokkaido Eastern Iburi earthquake are investigated. In particular, relation between the spatial distribution of high-frequency seismic waves and the attenuation structure of Hokkaido and northeastern Japan is focused on. Kakehi (2015) [2] studied the relation between the strong ground motion data from the intraslab and interplate earthquakes off Fukushima prefecture in northeastern Japan and the attenuation structure of the northeastern Japan, and found that the amplitude of high-frequency waves in the backarc side of the island arc becomes small due to the attenuation of the seismic waves propagating in the low-Q medium beneath the volcanic front and in the backarc side. In this study, relation between the spatially-biased distribution of strong ground motion data and the heterogeneous attenuation structure is investigated, as was done in Kakehi (2015) [2], with the earthquakes in Hokkaido as target of investigation. In order to investigate the effect of the source depth on the spatially-biased distribution of strong ground motion data, in addition to the observed data of the 2018 Hokkaido Eastern Iburi earthquake (called "event 1" hereafter), strong ground motions from two other deeper earthquakes, the 2015 interplate earthquake ($M_W$ 6.1, 66.07 km depth, called "event 2") and the 2007 intraslab earthquake ($M_W$ 5.5, 126.18 km depth, called "event 3"), are also analyzed.

For the analysis, high-quality strong ground motion data observed by the high-density strong ground motion observation networks, K-NET (Kinoshita, 1998 [3]) and KiK-net (Aoi et al., 2000 [4]) of National Research Institute for Earth Science and Disaster Prevention (NIED), Japan, are used.

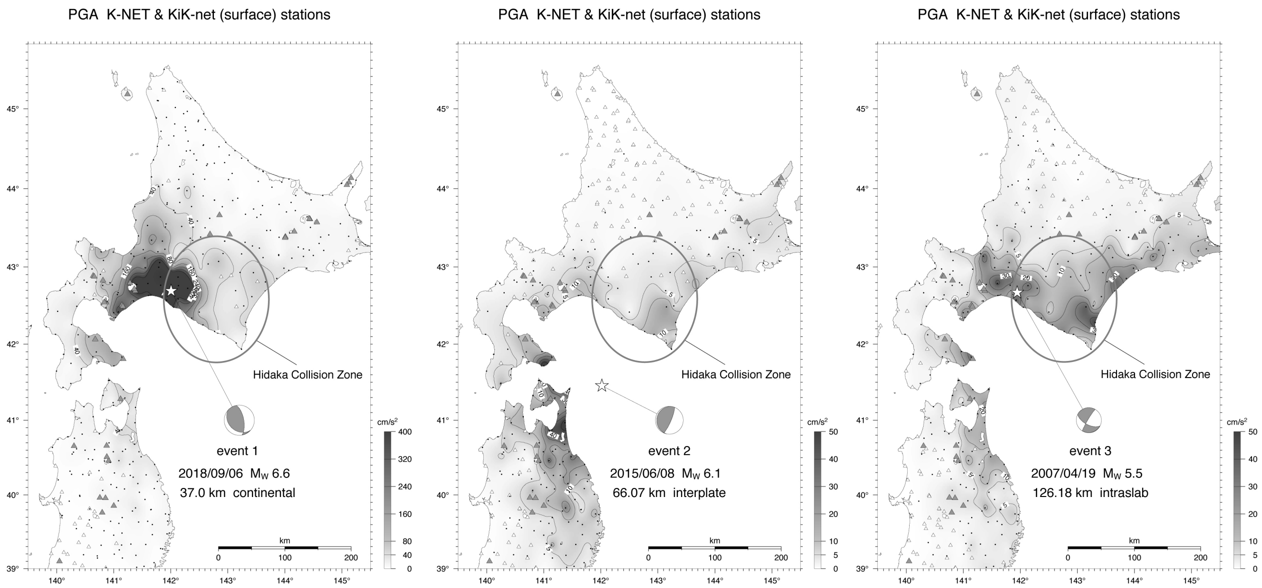


Fig. 1 – Spatial distributions of peak ground acceleration (PGA) of the three events with different focal depths: event 1 (2018/09/06, $M_W$ 6.6, 37.0 km depth), event 2 (2015/06/08, $M_W$ 6.1, 66.07 km depth), and event 3 (2007/04/19, $M_W$ 5.5, 126.18 km depth). White triangles are the stations without records. Hidaka collision zone is shown with an ellipse.

## 2. Spatial Distribution of Peak Ground Accelerations

First, spatial distributions of peak ground accelerations (PGA) of the three events are investigated. Fig. 1 shows the PGA distributions of the three events. For the deeper two events, event 2 and 3, clear contrast is seen between the acceleration amplitudes on the forearc side and those of the backarc side, i.e., the amplitudes on the backarc side are obviously small compared with those of the forearc side. On the other hand, in the case of event 1, whose focal depth is the shallowest among the three events, the amplitude contrast between the forearc and backarc sides is not clear, and the large acceleration area near the epicenter is striking. Additionally, between the two deep events, the contrast of event 3 with deeper focal depth is clearer.

In the region of Hokkaido and northeastern Japan, the island arc is bent in the western area of Hokkaido island. The direction of extent of the island arc is close to East-West in Hokkaido, while it is North-South in northeastern Japan. The amplitude contrast between the forearc and backarc sides seen in event 2 and 3 is clear both in Hokkaido and in northeastern Japan. In Hokkaido, however, an area with small amplitudes is exceptionally seen in the western side of Hidaka collision zone though the area is located in the forearc side. Small-amplitude area is also seen in case of the shallowest event 1, though it is not so clear as those of the two deeper events.

## 3. Acceleration Waveform Profile And PGA Attenuation Relation

Since K-NET and KiK-net networks have high station-density, it is possible to form a linear station array by picking up stations distributed almost linearly and trace seismic wave propagation along the linear array. Figures 2, 3, and 4 show the wave propagation along the linear array, with the vertical axis being the distance along the linear array (called "acceleration waveform profile" hereafter). Three linear arrays, line 1, 2, and 3, are picked commonly for the three events, as shown in the figures. Line 1 is a line extending eastward from the epicenter of event 1 in the forearc side of Hokkaido. Line 2 is a line extending from the forearc side to the backarc side, crossing over the volcanic front, in Hokkaido. Line 3 is a line extending southward in the forearc side of northeastern Japan. In the figures, EW component of acceleration waveforms is shown. The amplitudes can be relatively compared among the stations. Figure 5, 6, 7 show the PGA attenuation relation of the three events, where the horizontal axis is hypocentral distance and the vertical axis is PGA. In the figures of PGA attenuation relation, the plots of the stations included in the three linear arrays, line 1-3, are high-lighted with black circles in the respective panels. Solid line in the figure of attenuation relation is the PGA values predicted from magnitude, focal depth, and earthquake type based on the prediction formula of attenuation relation by Si and Midorikawa (1999) [5] and dashed lines shows +/- one standard deviation.

Using these figures of acceleration waveform profile and PGA attenuation relation, characteristics of the spatial distribution of amplitudes of high-frequency seismic waves are now examined. Since the deeper events show more simple spatial distribution, as shown below, we will start with the deepest event 3. In the acceleration waveform profile of line 3, high-frequency seismic waves are observed to propagate to a large distance without significant decay. PGA attenuation relation shows that the data of line 3 form a group with the largest amplitudes in the whole dataset. For line 3, high-frequency seismic waves are observed to propagate to a large distance without significant decay both in the acceleration waveform profile and in the PGA attenuation relation. It is unnatural, however, the amplitudes of the stations with small hypocentral distances (HKD103, HKD102, TKCH11, and TKCH06) are about the same as or smaller than those of the stations with much larger distances. This point is discussed on in the next section. Acceleration waveform profile of line 2 shows that the amplitudes of the stations at the volcanic front and in the backarc side are dramatically smaller than that of the station IBUH02 in the forearc side, and rapid decay of high-frequency wave amplitudes in the backarc side is clearly seen. This feature appears clearly also in the PGA attenuation relation. The range of amplitude variation in the PGA attenuation relation is the largest among the three events. This means the amplitude contrast between the forearc and backarc sides in case of event 3 is the clearest among the three events.


 

Next, we will see event 2, which has medium depth among the three events. In the acceleration waveform profile of line 3, high-frequency seismic waves are observed to propagate to a large distance without significant decay. PGA attenuation relation shows that the data of line 3 form a group with the largest amplitudes in the whole dataset. This feature is common with that of event 3. For line 3, high-frequency seismic waves are observed to propagate to a large distance without significant decay both in the acceleration waveform profile and in the PGA attenuation relation. It is unnatural, however, the amplitudes of the stations with small hypocentral distances (HKD103 and TKCH11) are about the same as those of the stations with much larger distances. This feature is also common with that of event 3. In the acceleration waveform profile, the amplitudes of the stations of line 1 are systematically smaller than those of line 3. This is because the hypocentral distances of the stations of line 1 are systematically larger than those of line 3 (this comes from that the epicenter of event 2 is far from line 1 and close to line 3). The systematic difference between the hypocentral distances of line 1 and line 3 can be seen in the figures of the PGA attenuation relation. For line 2, the feature that the amplitudes of the stations in the backarc side are very small is common with event 3, but the point that the amplitude of the station IBUH02 in the forearc side is also small is different from the case of event 3. The range of amplitude variation in the PGA attenuation relation is medium among the three events.

Finally, we will see event 1. Since this has the shallowest depth among the three events, the large amplitudes of the stations close to the epicenter are extremely striking in the figures of the acceleration waveform profiles, and it becomes difficult to discuss on the amplitude contrast between the forearc and backarc sides. In the figures of PGA attenuation relations, however, difference of the features among the three linear arrays can be seen, though it is not so clear as in the cases of event 3 and 2. The data of line 3 form a group with the largest amplitudes in the whole dataset. This feature is common with those of event 3 and 2. Many of the stations of line 1 have large amplitudes, but stations with small amplitudes are also included. In line 2, the amplitudes of the stations at the volcanic front and in the backarc side are relatively small in the whole dataset. The range of amplitude variation in the PGA attenuation relation is the smallest among the three events.

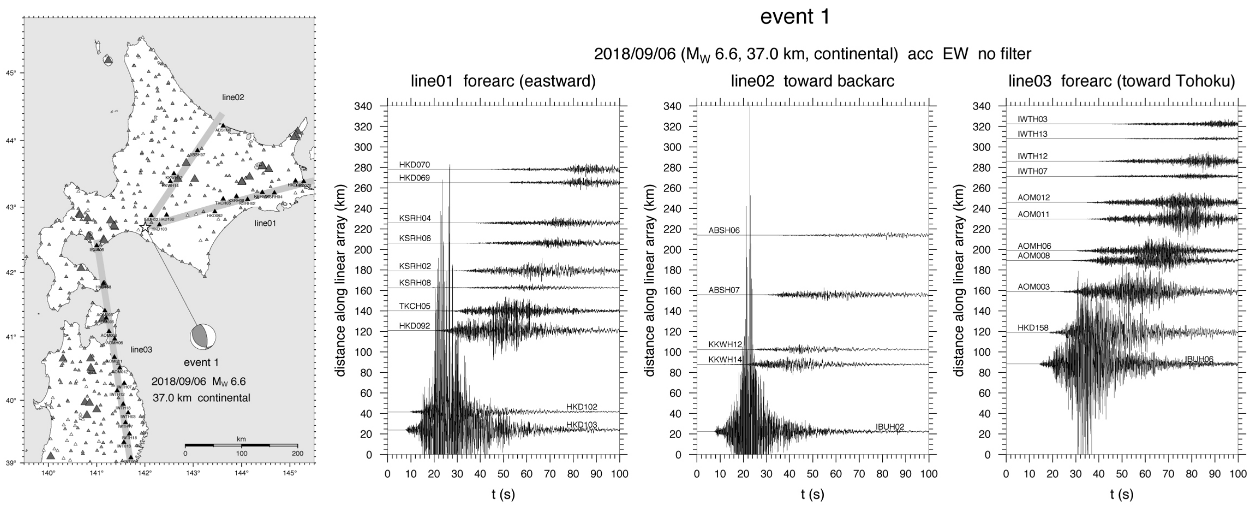


Fig. 2 – Acceleration waveform profiles along the three linear arrays (line 1-3) for the shallowest event 1.



 

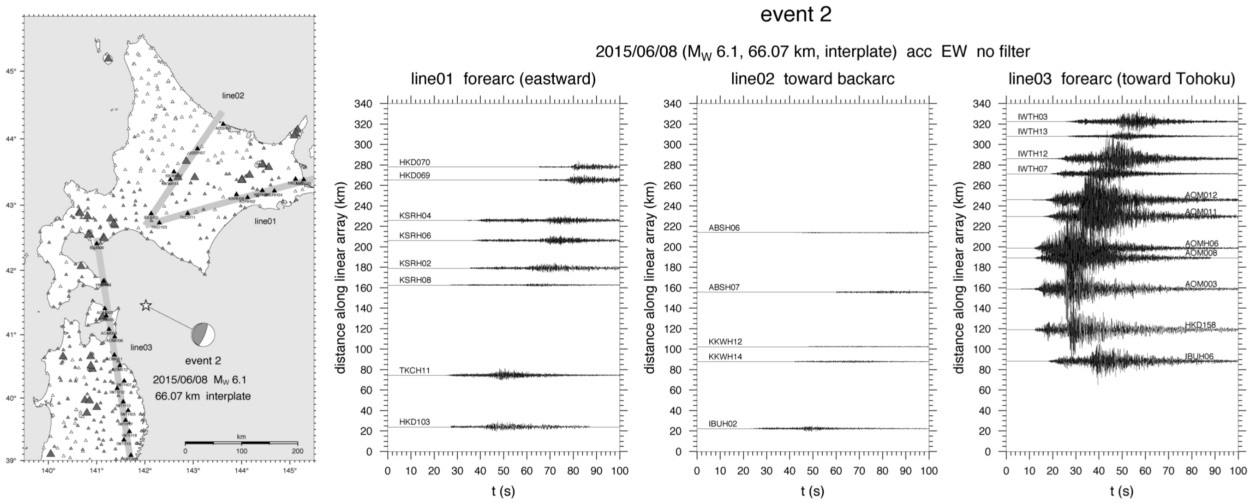


Fig. 3 – Acceleration waveform profiles along the three linear arrays (line 1-3) for event 2 with medium depth.

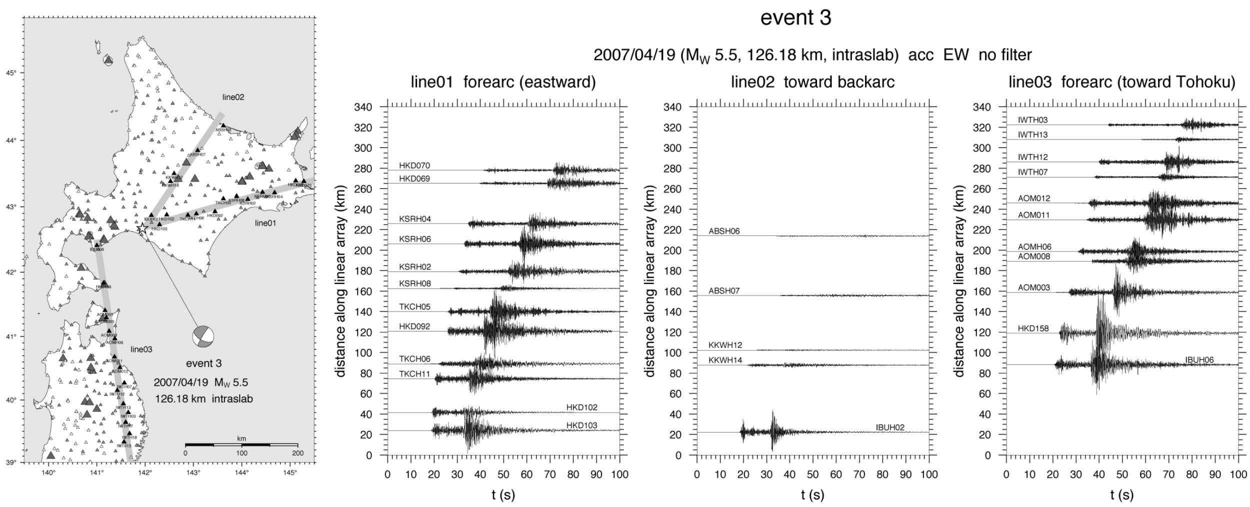


Fig. 4 – Acceleration waveform profiles along the three linear arrays (line 1-3) for the deepest event 3.



 

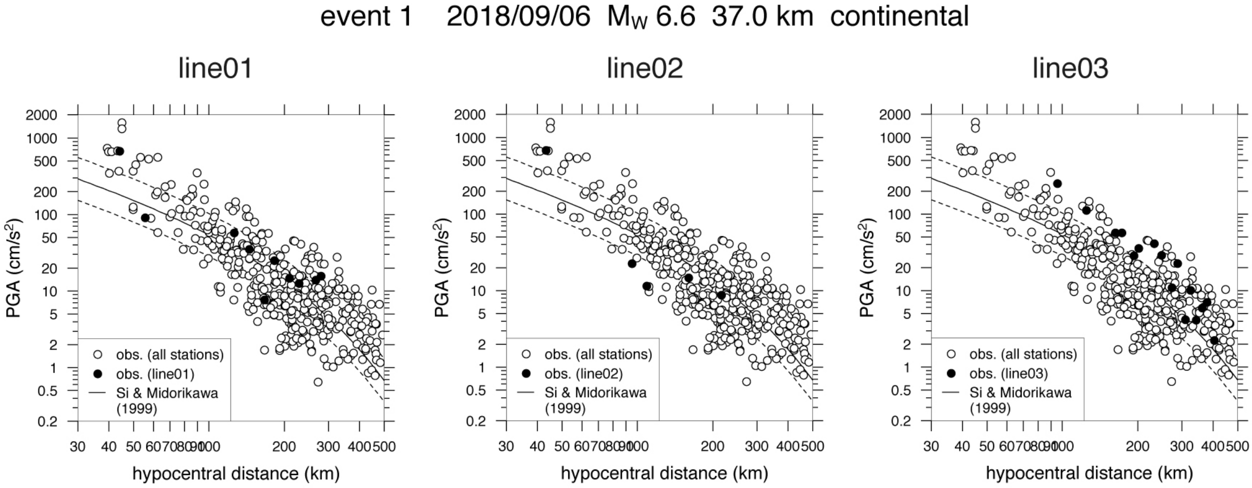


Fig. 5 – PGA attenuation relation for the shallowest event 1. In each panel, the stations included in each of the three linear arrays (line 1-3) are plotted with black circles and all the other stations are plotted with white circles. Prediced PGA values based on the formula by Si and Midorikawa (1999) [5] (solid line) and +/ one standard deviation (dashed lines) are also shown.

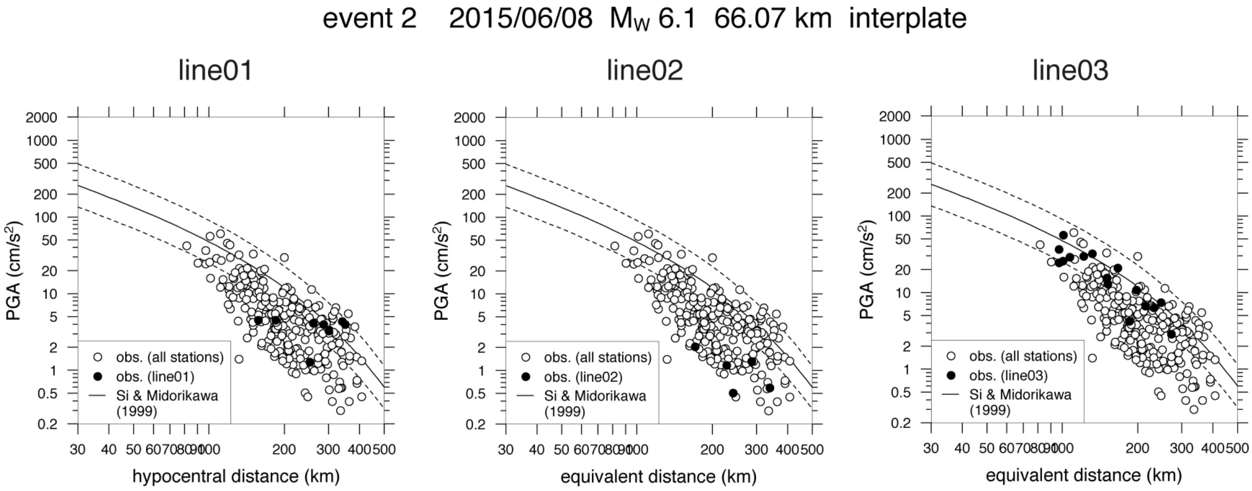


Fig. 6 – PGA attenuation relation for event 2 with medium depth. In each panel, the stations included in each of the three linear arrays (line 1-3) are plotted with black circles and all the other stations are plotted with white circles.



 

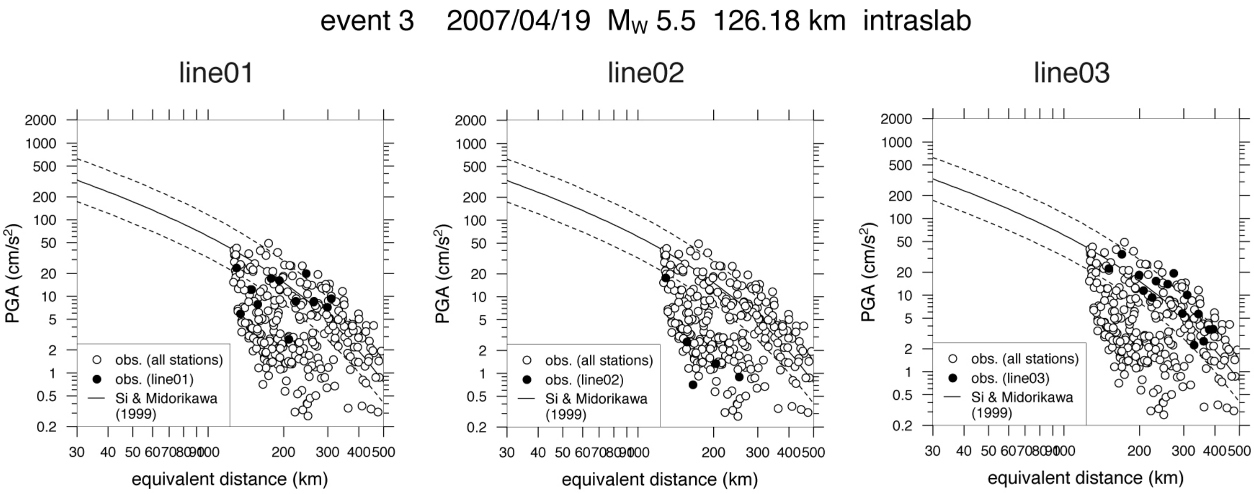


Fig. 7 – PGA attenuation relation for the deepest event 3. In each panel, the stations included in each of the three linear arrays (line 1-3) are plotted with black circles and all the other stations are plotted with white circles.

## 4. Discussion

First, the cause of the contrast of high-frequency wave amplitude between the forearc and backarc sides is examined. The attenuation structure of northeastern Japan and Hokkaido is investigated by the previous studies. Tsumura et al. (2000) [6] and Nakamura and Uetake (2004) [7] investigated the heterogeneous attenuation structure of northeastern Japan based on spectral inversion method, and both studies found the medium of backarc side of northeastern Japan has weak low-Q values and strong low-Q values are seen beneath the volcanoes. Kita et al. (2014) [1] and Nakamura and Shiina (2019) [8] reported that low-Q values are also seen in the backarc side and beneath the volcanoes in Hokkaido. The small amplitudes of high-frequency waves in the backarc side found commonly in the event 1-3 is comprehended to be due to the attenuation of seismic waves by propagating in the low-Q medium beneath the volcanic front and in the backarc side. Since the length of seismic wave path propagating in the low-Q region in the back arc side is longer for deeper event, the attenuation due to low-Q medium becomes stronger for deeper events. This can explain the contrast of high-frequency wave amplitude between the forearc and backarc sides is the most clear in the case of the deepest event 3 and the least clear in the case of the shallowest event 1.

Next, we will consider the effect of geometrical spreading factor. As the cause of the least clear contrast between the forearc and backarc sides seen in the case of the shallowest event 1, effect of spatial variation of geometrical spreading factor on the ground surface should be considered, in addition to the path-length effect in the low-Q region mentioned above. In case of shallow event, the geometrical spreading factor on the ground surface is large close to the epicenter and becomes small rapidly with distance from the epicenter, while the spatial variation of geometrical spreading factor on the ground surface is more gradual in case of deep event. This difference of spatial variation of geometrical spreading factor on the ground surface due to source depth brings the following effect. In case of deep event, the amplitude contrast originated from heterogeneous attenuation structure appears relatively directly, while it is masked considerably by the strong spatial variation of geometrical spreading factor. Figure 8 shows the spatial distributions of geometrical spreading factor on the ground surface for the three events. The spatial variation of geometrical factor of the shallowest event 1 is clearly much stronger than those of the deeper two events.

As mentioned in the previous section, an area with small amplitudes is exceptionally seen in the western side of Hidaka collision zone, commonly among three events, though the area is located in the forearc side of Hokkaido. In the previous studies by Kita et al. (2014) [1] and Nakamura and Shiina (2019) [8], low-Q region is found in the western side of Hidaka collision zone. Kita et al. (2014) [1] reported existence of low-$Q_P$ zone in the depth range of 0-60 km. Nakamura and Shiina (2019) [8] found low-$Q_S$ zone in the depth range of 0-40 km. This complex attenuation structure is maybe brought by the result of arc-arc collision process in Hidaka region. The exceptional area with small amplitudes in the western side of Hidaka collision zone is interpreted to be caused by the attenuation of seismic waves propagating in this low-Q zone in the forearc side. For event 2, as also mentioned in the previous section, the amplitude of the station IBUH02 in the forearc side is small, and this is not seen in the case of event 1 and 3. This is because the source location of event 2 is distant southward from the sources of event 1 and 3, which have very close epicenters. Therefore, the low-Q zone in the western side of Hidaka collision zone comes between the source and the station IBUH02 only in case of event 2, and the amplitude decay is interpreted to have been brought by the wave propagation in that low-Q zone.

In northeastern Japan, since the attenuation structure relatively simple, i.e., high-Q forearc side and low-Q back arc side, spatial distribution of high-frequency wave amplitudes also becomes relatively simple. On the other hand, in Hokkaido, since the attenuation structure is relatively complex due to the existence of the low-Q zone in the western side of Hidaka collision zone in the forearc side, the spatial distribution of high-frequency wave amplitudes also becomes relatively complex for all of the three events.

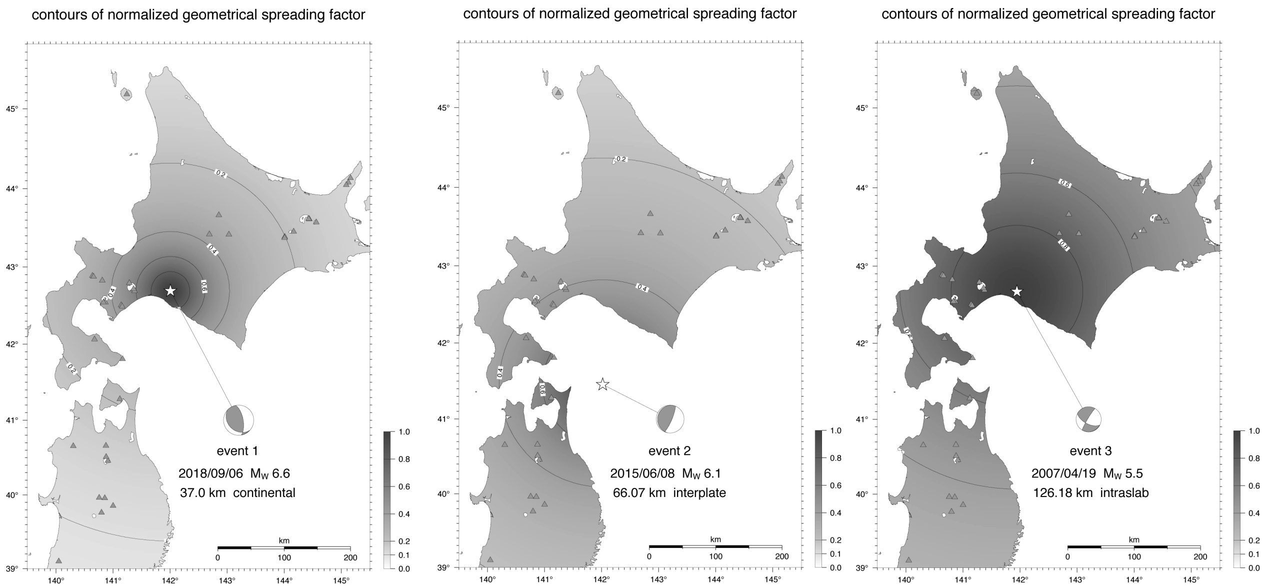


Fig. 8 – Spatial distributions of geometrical spreading factor of the three events with different focal depths (event 1-3) on the ground surface. The factor values are normalized with the maximum value (value at the epicenter) for each event.

## 5. Conclusion

Characteristics of the strong ground motions from the 2018 Hokkaido Eastern Iburi earthquake ($M_W$ 6.6, 37.0 km depth, event 1) are studied using the records of high-density strong ground motion observation network (NIED K-NET and KiK-net). In this study, spatial contrast of high-frequency seismic wave amplitude between the forearc and backarc sides of the island arc, caused by the decay of high-frequency waves in the backarc side due to propagating low-Q medium is focused on. For comparison, strong ground motions from two other deeper earthquakes, the 2015 interplate earthquake ($M_W$ 6.1, 66.07 km, event 2) and the 2007 intraslab earthquake ($M_W$ 5.5, 126.18 km, event 3), are also analyzed. From the analysis of the spatial distribution of PGA, trace of wave propagation along linear arrays, and PGA attenuation relation, the spatial contrast of high-frequency wave amplitude between the forearc and backarc sides is found to be clear for the two deeper events (event 2 and 3), but is not clear for the shallowest event 1. This result is interpreted by referring to the following two factors. The first factor is the path length of seismic waves propagating in low-Q medium in the backarc side. The path length of the shallowest event 1 is shorter than those of the two deeper events, and this makes the decay of high-frequency wave amplitude in the backarc side unclear for event 1. The second factor is the spatial variation of geometrical spreading factor. The spatial variation of geometrical spreading factor of the shallowest event 1 is stronger than those of the two deeper events. This works as a mask effect to the spatial contrast between the forearc and backarc sides originated from the heterogeneous attenuation structure in case of event 1. In Hokkaido, since the attenuation structure is relatively complex due to the existence of the low-Q zone in the western side of Hidaka collision zone in the forearc side, the spatial distribution of high-frequency wave amplitudes also becomes relatively complex for all of the three events.

## 6. Acknowledgements

The strong ground motion data recorded by K-NET and KiK-net of National Research Institute for Earth Science and Disaster Prevention, Japan, were used for the analysis. For the hypocenter and source mechanism information, the unified hypocenter catalogue by the Japan Meteorological Agency and the NIED F-net solution catalogue were referred to, respectively. GMT (Wessel and Smith, 1995 [9]) was used for drawing the figures.

## 7. References

[1] Kita S, Nakajima J, Hasegawa A, Okada T, Katsumata K, Asano Y, Kimura T (2014): Detailed seismic attenuation structure beneath Hokkaido, northeastern Japan: arc-arc collision process, arc magmatism, and seismotectonics. *J Geophys Re Solid Earth* **119**, do:10.1002/2014JB011099.

[2] Kakehi Y (2015), Characteristics of strong ground motions from intraslab and interplate earthquakes off Fukushima Prefecture, *Report of Research Center for Urban Safety and Security, Kobe Univ.*, **19**, 308-316.

[3] Kinoshita S (1998): Kyoshin Net (K-NET), *Seism Res Lett*, **69**, 309-332.

[4] Aoi S, Obara K, Hori S, Kasahara K, Okada Y (2000): New strong- motion observation network: KiK-net, *Eos Trans. AGU*, **81**(48), Fall Meet. Suppl, Abstract S71A-05.

[5] Si H, Midorikawa S (1999): New attenuation relationships for peak ground acceleration and velocity considering effects of fault type and site condition, *J Struct Constr Eng, AIJ*, **523**, 63-70. (in Japanese with English abstract)

[6] Tsumura N, Matsumoto S, Horiuchi S, Hasegawa A (2000): Three-dimensional attenuation structure beneath the northeastern Japan arc estimated from spectra of small earthquakes, *Tectonophysics*, **319**, 241-260.

[7] Nakamura R, Uetake T (2004): Three dimensional attenuation structure beneath the Tohoku district by using seismic strong motion records. *Zisin*, **56**, 447–455, doi:10.4294/zisin1948.56.4_447. (in Japanese with English abstract)

[8] Nakamura R, Shiina T (2019): Three-dimensional S-wave attenuation structure in and around source area of the 2018 Hokkaido Eastern Iburi Earthquake, Japan, *Earth, Planets and Space*, **71**:114, doi:10.1186/s40623-019-1095-6.

[9] Wessel P, Smith WHF (1995): New version of the Generic Mapping Tools released, *Eos Trans AGU*, **76**, 329.



 